Original Article

Dendritic cells serve as a "Trojan horse" for oncolytic adenovirus delivery in the treatment of mouse prostate cancer

Zhao-lun LI[1, #], Xuan LIANG[2, #], He-cheng LI[1], Zi-ming WANG[1], Tie CHONG[1, *]

[1]Department of Urology, the Second Affiliated Hospital, Xi-an Jiaotong University Medical College, Xi-an 710004, China; [2]Department of Oncology, the First Affiliated Hospital, Xi-an Jiaotong University Medical College, Xi-an 710061, China

Aim: Adenovirus-mediated gene therapy is a novel therapeutic approach for the treatment of cancer, in which replication of the virus itself is the anticancer method. However, the success of this novel therapy is limited due to inefficient delivery of the virus to the target sites. In this study, we used dendritic cells (DCs) as carriers for conditionally replicating adenoviruses (CRAds) in targeting prostate carcinoma (PCa).
Methods: Four types of CRAds, including Ad-PC (without PCa-specific promoter and a recombinant human tumor necrosis factor, rmhTNF, sequence), Ad-PC-rmhTNF (without PCa-specific promoter), Ad-PPC-NCS (without an rmhTNF sequence) and Ad-PPC-rmhTNF, were constructed. The androgen-insensitive mouse PCa RM-1 cells were co-cultured with CRAd-loading DCs, and the viability of RM-1 cells was examined using MTT assay. The *in vivo* effects of CRAd-loading DCs on PCa were evaluated in RM-1 xenograft mouse model.
Results: Two PCa-specific CRAds (Ad-PPC-NCS, Ad-PPC-rmhTNF) exhibited more potent suppression on the viability of RM-1 cells *in vitro* than the PCa-non-specific CRAds (Ad-PC, Ad-PC-rmhTNF). In PCa-bearing mice, intravenous injection of the PCa-specific CRAd-loading DCs significantly inhibited the growth of xenografted tumors, extended the survival time, and induced T-cell activation. Additionally, the rmhTNF-containing CRAds exhibited greater tumor killing ability than CRAds without rmhTNF.
Conclusion: DCs may be an effective vector for the delivery of CRAds in the treatment of PCa.

Keywords: prostate carcinoma; conditionally replicating adenoviruses; PSA; CD40L; recombinant human tumor necrosis factor; dendritic cells; RM-1 cells; xenograft mouse model

Introduction

Prostate carcinoma (PCa) is one of the most frequently diagnosed malignant tumors in elderly males[1]. Radical prostatectomy and radiation therapy are the commonly used clinical methods for the treatment of PCa. However, up to 40% of patients who are treated with surgery and radiation may eventually relapse[2], resulting in the migration of cancer cells to other areas of the body. Androgen-deprivation therapy is the preferred treatment for invasive and migratory PCa[3]. While PCa patients initially respond well to androgen deprivation, unfortunately, almost all patients will experience recurrence within 1–3 years due to the development of androgen-independent cancer cells[4]. Therefore, there is a clear clinical need for new methods that can control the recurrence, progression and metastasis of PCa.

Conditionally replicating adenoviruses (CRAds) are now being explored as cancer gene therapy delivery vehicles because they allow viruses to be replicated selectively in predetermined target tumor cells, thereby enhancing the spread of therapeutic gene expression and offering an optimal strategy for cancer treatment[5].

Almost all research into CRAd-mediated PCa gene therapy is limited to local PCa, owing to ease of administration by intratumoral injection and local copying in the prostate, which means that amplification produces fewer side effects. Obviously, intratumoral injection is no longer applicable for advanced PCa with distant metastasis to bone or other organs. Intravenous injection might be one option to solve this problem. However, the intravenous injection of CRAds has produced more difficulties. Because blood is a relatively closed and exclusive system, a series of non-specific and specific host

defenses removes virus particles from the circulation, producing a major obstacle to achieving effective systemic delivery[6]. Dendritic cells (DCs) are professional antigen-presenting cells (APCs) that play critical roles in the activation of antigen-specific naïve T cells[7] and the regulation of the innate immune response[8]. The ability of DCs to deliver CRAds to metastatic melanoma cancer cells *in vitro* and *in vivo* has been demonstrated in a previous report[6]. CD40 is highly expressed on the surface of DCs. The CD40-CD40 ligand (CD40L) interaction plays an important regulatory role aspects of in DC function such as T-lymphocyte activation and effector cytokine production[9]. Researchers have shown that arming an oncolytic virus with CD40L brings the tumor antigens to the DC surface by CD40L, thereby initiating more effective anti-tumor immunity[10].

In the present study, we fused the prostate-specific antigen (PSA) with CD40L and constructed PCa-specific CRAds. Using the DCs as CRAd carriers, the results suggested that CRAd-loading DCs have significant activity against PCa cells and may represent a promising new therapy for PCa.

Materials and methods
Animals, cells and cell culture
Male C57BL/6 mice (body weight: 16–18 g) at 4–6 weeks of age were obtained from Institute of Materia Medica, Chinese Academy of Medical Sciences & Peking Union Medical College (Beijing, China). The human transformed embryonic kidney (HEK)-293 cell line and an androgen-insensitive MHC class I-deficient mouse PCa cell line, RM-1, which is syngeneic in C57BL/6 mice[11], were obtained from the American Type Culture Collection (ATCC; Manassas, VA, USA). The cells were cultured in Dulbecco's minimum essential medium (MEM, Mediatech Inc; Manassas, VA, USA), containing 10% fetal bovine serum (FBS; Gemini Bioproducts; Woodland, CA, USA) and 1% antibiotic-antimycotic solution (Mediatech Inc; Manassas, VA, USA)[12] and were maintained at 37 °C in 5% CO_2 in a fully humidified incubator.

The protocols were approved by the Committee for Ethical Procedures of the Second Affiliated Hospital, Xi-an Jiaotong University Medical College, and the study was performed in accordance with the Declaration of Helsinki (2008) for humans.

Construction of Ad-PC, Ad-PC-rmhTNF, Ad-PPC-NCS and Ad-PPC-rmhTNF
The prostate-specific oncolytic adenovirus was prepared according to a previous report[5]. First, we designed and constructed a prostate-specific promoter PSAe-PSMAe-TARPp (PPTp), which comprised the prostate-specific antigen enhancer (PSAe), prostate-specific membrane antigen enhancer (PSMAe) and T-cell receptor g-chain alternate reading frame protein promoter (TARPp) in that order. Second, recombinant adenovirus Ad-PSA-CD40L-PPT was prepared using an oncolytic adenovirus preparation system, which was established by our laboratory. The fusion protein gene PSA-CD40L was constructed into a plasmid, and then this sequence was inserted into pShuttle-cmv to obtain pShuttle-PSA-CD40L. The helper plasmid TE-SV-PPT-IR-55K for oncolytic adenovirus preparation was constructed by replacing the TP gene of TE-SV-IR-TP-55K with PPTp. Thereafter, the restriction enzyme *Mfe* I was used to cut TE-SV-PPT-IR-55K and obtain PPT-E1A, and then, the fragment was inserted into the pshuttle-PSA-CD40L in the forward direction to obtain the recombinant plasmid pshuttle-PSA-CD40L-PPT-E1A. Finally, the immune and oncolytic adenovirus Ad-PPT-PSA-CD40L (Ad-PPC) was prepared using the Adeasy system (Agilent Technologies, Santa Clara, CA, USA). Ad-PPC was purified by density gradient centrifugation of cesium chloride. The same method was used to obtain the control adenovirus Ad-PSA-CD40L (Ad-PC).

The TNF mutant (recombinant mutated human TNF; rmhTNF) was prepared according to a previous report[13]. Briefly, the primers were designed according to TNF-α (GenBank) (Table 1), using the rhTNF-α gene as a template, with amplification of the rmhTNF sequence being achieved by overlap PCR. Double digestion of the IRES from the plasmid pIRES-EGFP was performed, and then mhTNF and a nonsense control sequence (NCS) were connected to IRES. The latter was inserted into the adenovirus Ad-PPC backbone plasmid, and then the resultant plasmid was linearized using the restriction enzyme *Pac* I before liposomes were transfected into HEK293 cells to obtain the CRAds, Ad-PPC-rmhTNF and Ad-PPC-NCS. The prostate-specific promoter PPT-free control CRAd Ad-PC-rmhTNF was constructed synchronously. All of the recombinant adenoviruses are shown in Figure 1.

Table 1. Primers for overlap PCR.

| Number	Primers	
1	*TGG AAT TCA TGT CTC GAA CCC GTA AAC GTA AG*	Containing the initiation codon and *Eco*R I recognition sequence, replacing the CCG which encode the eighth amino by CGT, replacing AGT which encode the ninth amino by AAA, replacing GAT which encode the ninth amino by CGT.
2	*ACC CGT AAA CGT AAG CCT GTA GCC CAT GTT*	Partly overlap with primer 1
3	*GTG GTC GAA CGA TCG GGC CAA TGC CCT CC*	Replacing the CTG which encode the twenty-ninth amino by TCG, replacing CGC which encode the thirty-first amino by GAT.
4	*CGA TCG TTC GAC CAC TGG AGC TGC CCC T*	–
5	*TCA AAA GGC AAT GAT CCC AAA G*	Replacing the TAA which encode the one hundred and fifty seventh amino by AAA, and containing termination codon and *Bam*H I recognition sequence
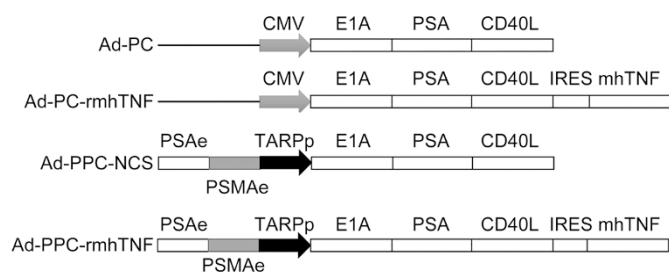
Figure 1. Schematic outline of the recombinant adenoviruses. CMV, immediate-early human cytomegalovirus promoter; E1A, E1A coding sequence; PSA, PSA coding sequence; CD40L, CD40L coding sequence; PSAe, PSA enhancer; PSMAe, PSMA enhancer; TARPp, TARP promoter; IRES, IRES coding sequence; mhTNF, human TNF-α coding sequence.

Murine DC-loaded CRAds

The generation of bone marrow-derived DCs was performed as described previously[14]. Femur and tibia marrow cells from C57BL/6 mice were depleted of erythrocytes using red blood cell lysis buffer (Sigma-Aldrich, St Louis, MO, USA). The cells were then cultured in complete RPMI-1640 media containing 10% fetal bovine serum, 10 ng/mL GM-CSF and 10 ng/mL IL-4. On d 2, the floating cells were discarded, and the adherent cells were replenished with fresh complete media. On d 4, the culture supernatants were collected and centrifuged, and the cell pellets were resuspended in fresh RPMI-1640 before being returned to the original plate. On d 6, adherent DCs were incubated with B16-F10 cell lysate (50 μg/mL) for 24 h and then were matured by the addition of 1 μg/mL lipopolysaccharide (Sigma-Aldrich) for 24 h. Mature DCs were harvested and phenotypic markers, such as MHC II, CD80 and CD86 of DCs, were confirmed by fluorescence-activated cell sorting analysis. For the DC-loaded CRAd experiments, 1×10^6 DCs were infected with 0, 5, 10, 50, 100, 200 MOI of CRAd attached with green fluorescent protein (GFP). Ad-PC, Ad-PC-rmhTNF, Ad-PPC-NCS and Ad-PPC-rmhTNF ($n=10$) were suspended in 100 μL of PBS. After 24 h of infection, the infection efficiency was detected by fluorescence detection.

Establishment of a mouse PCa model

Mouse PCa models were generated by the injection of 0.2 mL of 5×10^6/mL RM-1 cells into the flanks of male C57BL/6 mice. After tumors were grown for at least 2 weeks after implantation, 40 mice were randomly divided into 4 different treatment groups (10 mice in each group), and 1×10^6 DCs, which had been infected with 200 MOI of Ad-PC ($n=20$), Ad-PC-rmhTNF ($n=20$), Ad-PPC-NCS ($n=20$) or Ad-PPC-rmhTNF ($n=20$) suspended in 100 μL of PBS, were intravenously injected into the lateral tail vein. Ten other mice were selected as positive controls and were injected with 100 μL of PBS 2 weeks after tumor implantation. Fourteen days after CRAd or PBS injection, the tumor volumes of each group were measured to assess the effect of DCs loaded with CRAds on tumor growth. The tumor volume was calculated using the following formula: $v=l \times b^2/2$, where l indicates the long diameter, and b indicates the short diameter. Additionally, survival analysis was performed using the Kaplan-Meier method.

Cell viability and proliferation

DC viability after isolation was determined using the standard Trypan blue exclusion test (Sigma-Aldrich, St Louis, MO, USA). The total number of viable and nonviable cells was counted using a Bürker counting chamber, and the percentage of viable cells was calculated. The RM-1 viability and peripheral blood mononuclear cell proliferation were measured using the MTT assay. Briefly, the cells were seeded into 96-well plates and washed twice with PBS, and 10 μL of MTT was added to each well. Next, the cells were incubated at 37 °C for 2 h, and 100 μL of DMSO was added to dissolve the formazan crystals. The absorbance was measured at 560 nm using a Spectra Max Paradigm Multi-Mode Reader (Molecular Devices, Austria). The proliferation of peripheral blood mononuclear cells was also studied using the intracellular expression of the nuclear Ki-67 antigen (BD Pharmingen) by flow cytometric analysis. In each assay, 5×10^5 mononuclear cells were incubated with 100 μL of cytofix/cytoperm (BD Pharmingen) for 15–20 min on ice. The cells were washed twice with perm/wash buffer (BD Pharmingen) and incubated with an anti-Ki-67 PE antibody (or the matched isotype control) diluted in perm/wash buffer for 30 min on ice in the dark. Next, the cells were washed again with the perm/wash buffer, resuspended in PBS and analyzed by flow cytometry. The values are expressed as the percentage of stimulated cells positive for the Ki-67 mAb corrected for the percentage of stimulated cells that were positively stained by the isotype control.

Mouse spleen T-cell subset analysis

Mouse spleen cell suspensions were prepared from spleen samples. The spleen cells were applied to nylon wool columns, and T cells were collected as previously described[15]. Mouse spleen T cell subset analysis was performed by double staining with APC and PE (BD Biosciences, San Diego, CA, USA). Spleen T cells were incubated with APC-conjugated anti-CD4 and PE-conjugated anti-CD8. After an incubation period of 15 min, the cells were analyzed on a flow cytometer (FACSCanto II; BD Biosciences). The percentages of cells expressing CD4 and CD8 were then calculated.

Surface markers

The surface markers of DCs were detected by flow cytometry. The cells were detached with trypsin-EDTA (Invitrogen) and resuspended in PBS containing 1% BSA and 0.1% sodium azide. The samples were incubated for 1 h on ice with anti-CD80, anti-CD86 and anti-MHC II antibodies (Abcam, Cambridge, UK). After washing with PBS, cell staining was carried out for another 1-h incubation with fluorescent anti-rabbit immunoglobulin G (Abcam, Cambridge, UK). The stained cells were analyzed on a FACSCalibur 440E (Becton Dickinson) using Cell Quest software (BD Biosciences Immunocytometry Systems).

Survival analysis

Two weeks after RM-1 injection (as described above), the mice were injected intravenously in the lateral tail vein with or without 1×10^6 DCs that had been infected with 200 MOI of Ad-PC, Ad-PC-rmhTNF, Ad-PPC-NCS or Ad-PPC-rmhTNF (*n*=10) suspended in 100 μL of PBS. Mice treated with PBS served as positive controls. All of the mice were followed daily until death.

Statistical analysis

Data are presented as the mean±standard error (SEM) of the data points. Statistical analysis was performed using Student's *t*-test or one-way ANOVA followed by *post-hoc* tests and LSD using SPSS 19.0 software. Survival analysis was performed using the Kaplan-Meier method. Data were considered to be statistically significant at a *P* value less than 0.05.

Results

Identification of the load efficiency and safety of CRAds on DCs

One prerequisite for exploiting DCs as carriers for CRAds is to identify a CRAds agent that combines a maximum load efficiency with minimum toxicity for DC viability. Therefore, we sought to identify an exact dose of CRAds for DC loading using gradually increasing concentrations of virus. In our experiments, four types of CRAds, including Ad-PC (without a PCa-specific promoter and rmhTNF sequence), Ad-PC-rmhTNF (without a PCa-specific promoter), Ad-PPC-NCS (without a rmhTNF sequence) and Ad-PPC-rmhTNF, were constructed as described in the Materials and methods section, and the DCs were infected with various doses (0, 5, 10, 50, 100 or 200 MOI) of these viruses. At 24 h after the infection, the fluorescence intensity in each group was detected under a fluorescence microscope. As shown in Figure 2A, the fluorescence intensity in CRAd-infected DCs increased in a dose-dependent manner despite the different types of viruses. Notably, the percentage of GFP-positive cells accounted for up to a maximum amount of 90% when the DCs were infected with 200 MOI of CRAds. Additionally, no significant difference in the infection efficiency was found among the four groups of DCs infected with the different types of CRAds. Furthermore, we
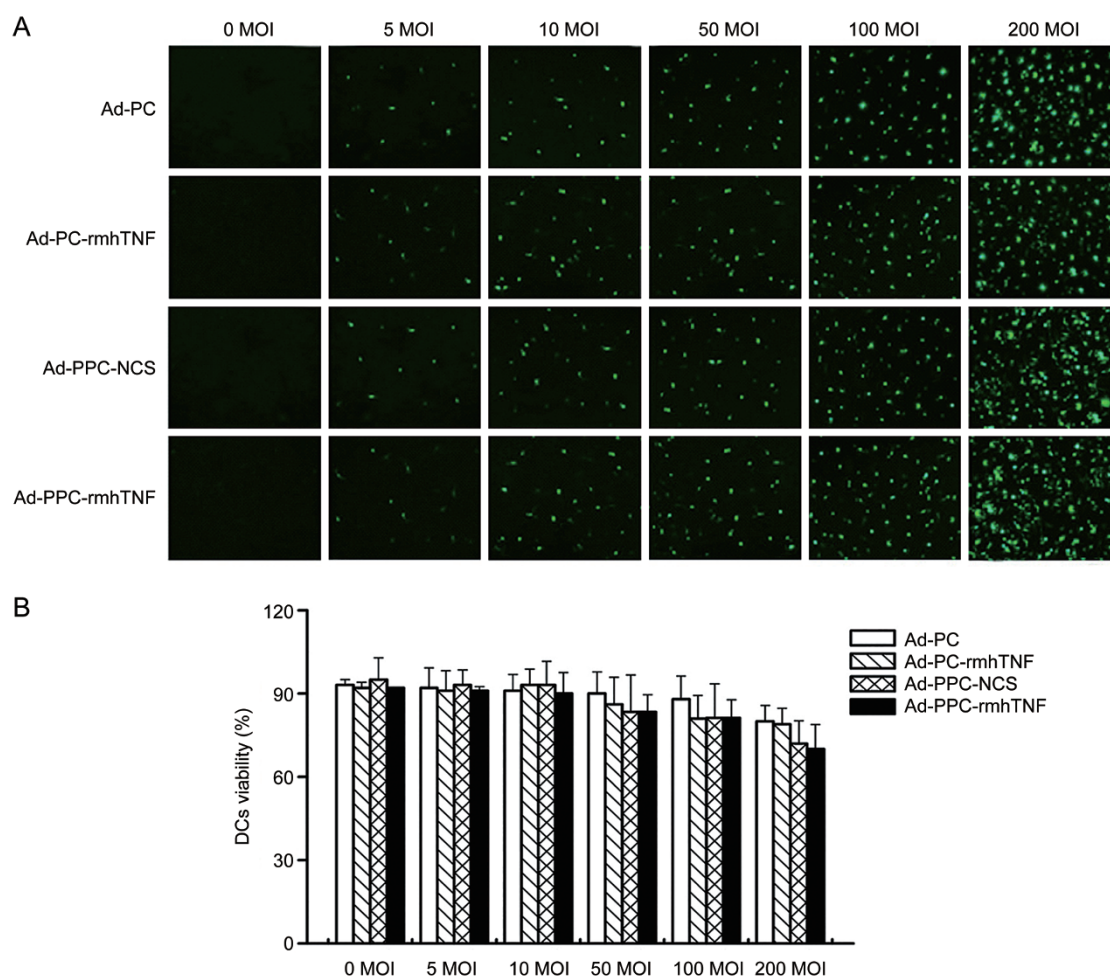

Figure 2. The infection efficiency and oncolysis effect of GFP-attached CRAds on DCs *in vitro*. (A) Fluorescence microscopy was performed to detect GFP expression in DCs after infection with 0, 5, 10, 50, 100 and 200 MOI of CRAds for 24 h. (B) DC viability after infection with 0, 5, 10, 50, 100 and 200 MOI of CRAds for 24 h.

determined the effects of these four CRAds on the viability of DCs using the MTT assay. The results showed that after infection with 0 to 200 MOI of CRAds, the viability of DCs did not alter significantly (Figure 2B). Therefore, the dose of 200 MOI was appropriate for CRAd infection with limited toxicity on DCs. Based on these data, we selected this dose of CRAd for DC loading in our subsequent experiments.

Effect of CRAd loading on DC maturation

DCs present antigens to naïve T lymphocytes, contributing to the initiation, suppression or termination of the adaptive immune response[16]. DC maturation is critical for antigen presentation and is characterized by the high expression of major histocompatibility complex class II (MHC II) and costimulatory molecules, including CD80 and CD86, *etc*[17, 18]. MhTNF-α, a recombinant and mutant TNF-α, has been reported to accelerate DC maturation with low toxicity to organisms. To compare the effects of CRAds with or without the mhTNF-α sequence on DC maturation, MHC II, CD80 and CD86 expression in CRAd-infected DCs was analyzed. As shown in Figure 3A, mhTNF-α expression was higher in cells infected with Ad-PC-rmhTNF or Ad-PPC-rmhTNF than in cells infected with Ad-PC or Ad-PPC-NCS. Accordingly, the results showed that the expression of MHC II, CD80 and CD86 was not significantly different between Ad-PC- and Ad-PPC-NCS-loaded DCs (Figure 3B, 3C and 3D). Compared with Ad-PC and Ad-PPC-NCS infection, infection with Ad-PC-rmhTNF and Ad-PPC-rmhTNF significantly elevated the expression of MHC II, CD80 and CD86, suggesting that mhTNF-α expression after CRAd infection promotes DC maturation (Figure 3B, 3C and 3D).

Oncolysis of PCa by CRAd-loaded DCs *in vitro*

To investigate the effect of these four groups of CRAd-loaded DCs on the viability of the prostate cancer cell line RM-1, we detected the expression of the PSA-CD40L fusion protein and mhTNF-α in RM-1 cells by flow cytometry and determined cell viability after coculturing with CRAd-loading DCs by the MTT assay. As shown in Figure 4A, RM-1 cells co-cultured with non-specific CRAd (Ad-PC or Ad-PC-rmhTNF)-loading DCs exhibited low PSA-CD40L expression. However, after co-culturing with Ad-PPC-NCS- or Ad-PPC-rmhTNF-loading DCs, the percentage of PSA-CD40L+ RM-1 cells increased in a dose-dependent manner (Figure 4A). The percentage of mhTNF+ cells remained unchanged after co-culturing with Ad-PC- or Ad-PPC-NCS-loading DCs but was increased by co-culturing with Ad-PC-rmhTNF-DCs (Figure 4B). Additionally, the results of the MTT assay showed that RM-1 cells were more sensitive to Ad-PPC-NCS- and Ad-PPC-rmhTNF-loading DCs than to those with non-PPT promoter-containing CRAds (Ad-PC and Ad-PC-rmhTNF); the most prominent oncolysis was attributed to Ad-PPC-rmhTNF-loading DCs (Figure 4C). These results demonstrated that Ad-PPC-NCS- and Ad-PPC-rmhTNF-loading DCs exhibited the most efficient cytotoxicity on RM-1 cells.

CRAd-loaded DCs influence tumor growth and the survival of tumor-bearing mice

Tumor volume is an important prognostic factor for PCa[18]. To determine the effect of CRAd-loading DCs on PCa growth in mice, we measured the volume of PCa in mice that were treated with PBS or Ad-PC-, Ad-PC-rmhTNF-, Ad-PPC-NCS-, or Ad-PPC-rmhTNF-loading DCs. After treatment, the tumor
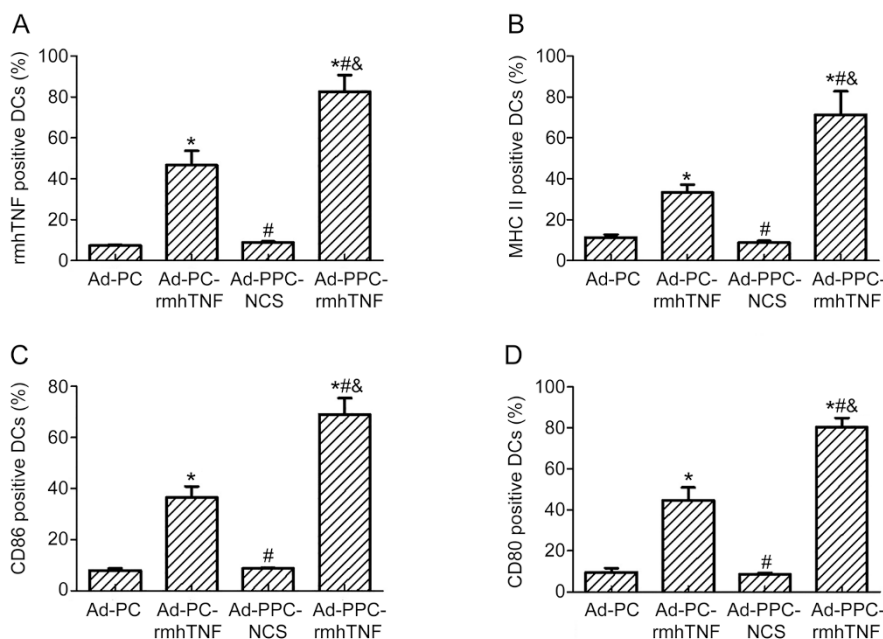

Figure 3. Analysis of surface markers of DCs after infection with 200 MOI of CRAds for 24 h. The percent of rmhTNF- (A), MHC II- (B), CD86- (C) and CD80-positive (D) DCs were detected by fluorescence microscopy. $^*P<0.05$ compared with Ad-PC, $^\#P<0.05$ compared with Ad-PC-rmhTNF, $^\&P<0.05$ compared with Ad-PPC-NCS.
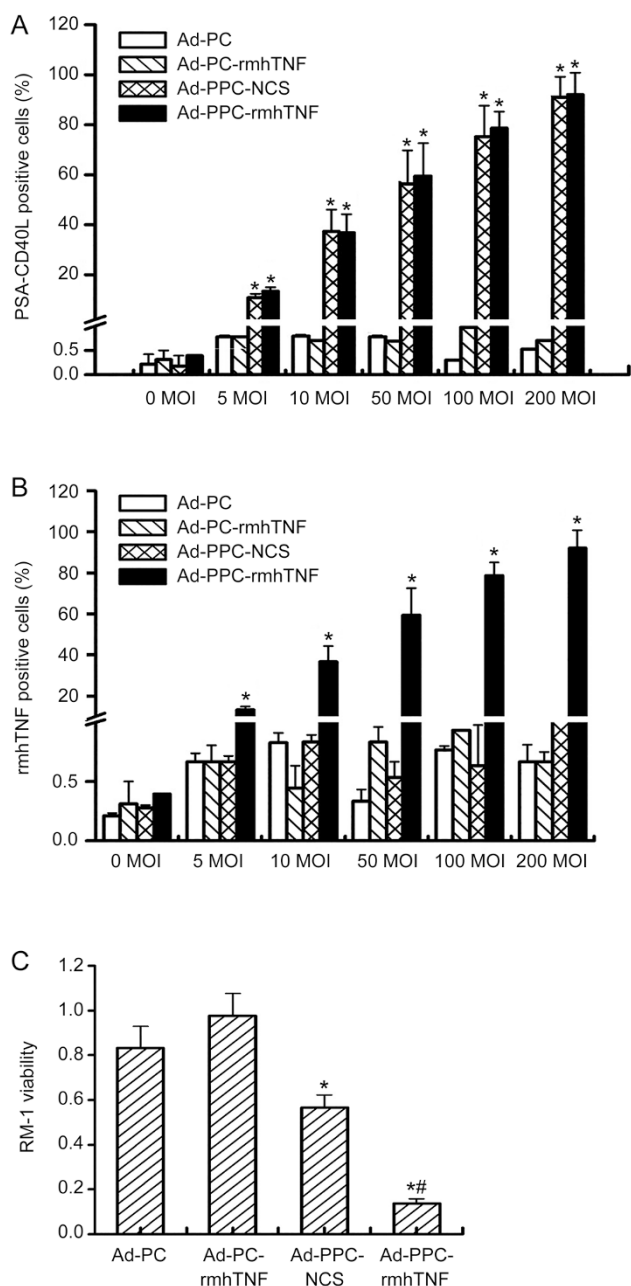
Figure 5. Effect of the intravenous injection of CRAd-loading DCs on prostate tumor volume and mouse survival. (A) Tumor volume after the treatment of mice with CRAd-loading DCs. (B) Mouse survival after the intravenous injection of CRAd-loading DCs. *$P<0.05$ compared with the control. #$P<0.05$ compared with Ad-PC. &$P<0.05$ compared with Ad-PPC-NCS.

PPC-rmhTNF-loading DCs survived for significantly longer ($P<0.05$) than those treated with PBS or Ad-PC- or Ad-PC-rmhTNF-loading DCs (Figure 5B). Moreover, treatment with Ad-PPC-rmhTNF-loading DCs resulted in a greater survival benefit than treatment with Ad-PPC-NCS-loading DCs (Figure 5B). Thus, these results indicated that the delivery of CRAd-loading DCs was efficient for the suppression of tumor growth and improvement of the survival of PCa-bearing mice.

The administration of CRAd-loading DCs activates T cells and reduces PCa growth

Finally, we examined whether CRAd-loading DCs would activate the immune response of PCa-bearing mice by measuring the differentiation of spleen CD4+ and CD8+ T cells. The results showed that Ad-PPC-NCS- and Ad-PPC-rmhTNF-loading DCs could increase the proportion of CD4+ T lymphocytes (Figure 6A) and the CD4+/CD8+ ratio (Figure 6B) compared with the control and Ad-PC-loading DCs ($P<0.05$). Moreover, Ad-PPC-rmhTNF-loading DC injection induced a higher CD4+/CD8+ ratio than Ad-PPC-NCS-loading DC injection (Figure 6A and 6B). Next, we determined the viability of RM-1 cells incubated with spleen T lymphocytes from mice treated with different CRAd-loading DCs. As shown in Figure 6C, T lymphocytes from mice treated with Ad-PPC-NCS- or Ad-PPC-rmhTNF-loading DCs significantly decreased RM-1 cell viability compared with lymphocytes from mice treated

Figure 4. Efficiency and oncolysis effect of four CRAds on RM-1 *in vitro*. Expression of the fused protein PSA-CD40L (A) and rmhTNF (B) in RM-1 cells after infection with 0, 5, 10, 50, 100 and 200 MOI of CRAds for 24 h. (C) Oncolysis effect of 200 MOI of different CRAds on RM-1. *$P<0.05$ compared with Ad-PC. #$P<0.05$ compared with Ad-PPC-NCS.

volumes in the Ad-PPC-NCS and Ad-PPC-rmhTNF groups were significantly smaller ($P<0.05$) than those in the control, Ad-PC and Ad-PC-rmhTNF groups (Figure 5A). Moreover, treatment with Ad-PPC-rmhTNF-loading DCs resulted in greater tumor growth inhibition than treatment with Ad-PPC-NCS-loading DCs (Figure 5A). We next tested whether CRAd-loading DCs improved the survival of PCa-bearing mice. As shown in Figure 5B, mice treated with Ad-PPC-NCS- or Ad-
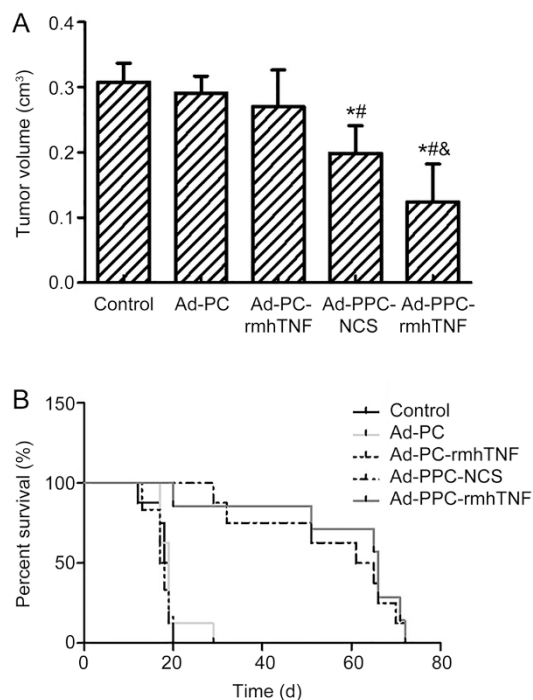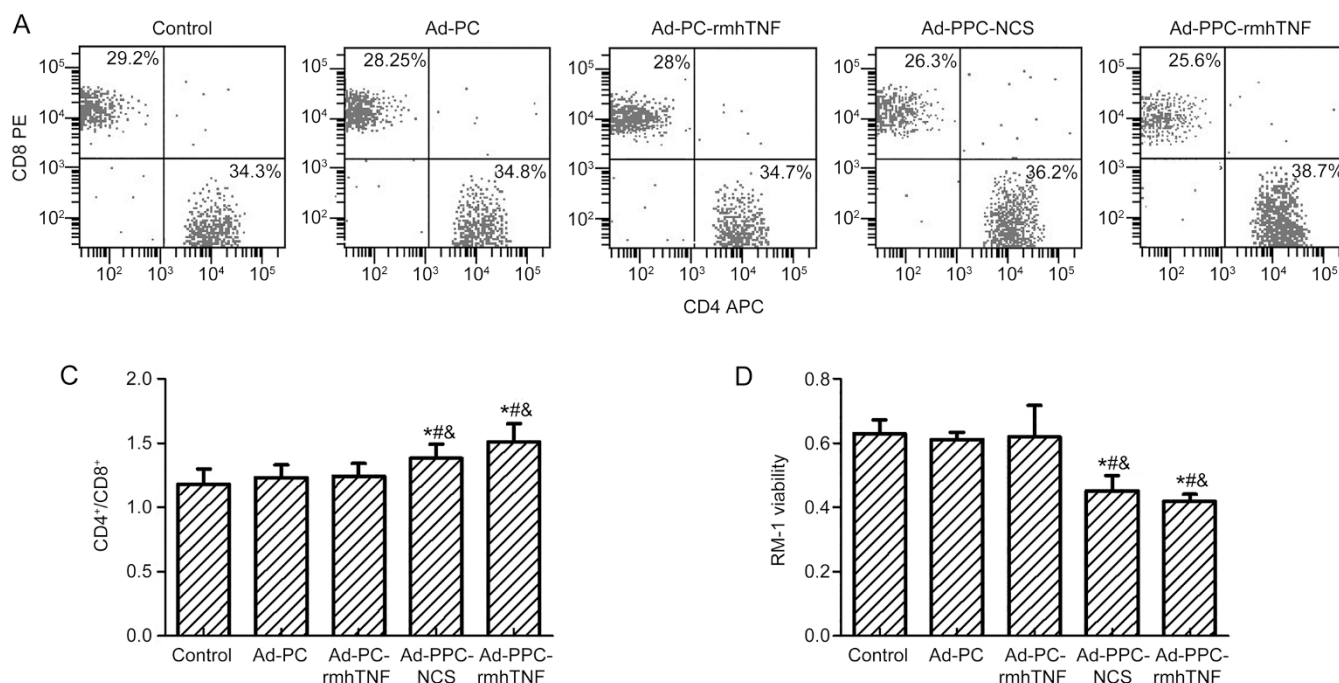
Figure 6. The effect of CRAd-loading DCs on mouse spleen T-lymphocyte subtype and tumor killing ability *in vitro*. (A) Spleen T-lymphocyte subtype analysis by flow cytometry. (B) CD4$^+$/CD8$^+$ ratio of spleen T lymphocytes. (C) RM-1 viability after incubation with spleen T lymphocytes. $^*P<0.05$ compared with the control. $^\#P<0.05$ compared with Ad-PC. $^\&P<0.05$ compared with Ad-PC-rmhTNF.

with PBS or Ad-PC- or Ad-PC-rmhTNF-loading DCs.

Discussion

CRAds are self-replicating, tumor-selective viruses that can directly lyse cancer cells. The efficiency of these agents has been confirmed by evidence from clinical trials[6]. CRAd therapy offers an attractive complementary strategy for localized prostate cancer because CRAds can be administered easily by intratumoral injection and local amplification in the prostate produces relatively few side effects[5]. However, the intratumoral injection of CRAds is ineffective for metastatic tumors[6]. Using cellular carriers to deliver CRAds will be a choice that can overcome a series of host defenses that remove virus particles from the circulation. DCs are professional APCs and play critical roles in the activation of antigen-specific naïve T cells and in the regulation of the innate immune response[8]. The ability of DCs to deliver CRAds to metastatic melanoma cancer cells *in vitro* and *in vivo* has been investigated in a previous study[6].

Regarding virotherapy, our CRAds were designed to address the biological requirements of PCa. Enhancement of the specificity of CRAds was achieved by constructing a PCa-specific promoter, PPTp, which comprised the prostate-specific antigen enhancer (PSAe), prostate-specific membrane antigen enhancer (PSMAe) and TARPp. The TP gene of the helper plasmid TE-SV-IR-TP-55K was replaced with PPTp. This CRAd has been shown to exhibit superior infectivity and tumor-selective replication in hormone-dependent and hormone-independent prostate cancer[5].

When exploiting DCs as cellular carriers for CRAds, it is important to consider how to limit viral activity in the carrier cells before the DCs reach the prostate cancer cells. In our study, we selected 200 MOI of CRAds because this amount of virus exhibited limited DC cytotoxicity. We demonstrated that DC-based viral delivery had an oncolytic effect on PCa, activated the immune response, and increased the survival of tumor-bearing animals. These results validated the feasibility of using DCs as cellular carriers for CRAds.

TNF-α is a cytokine produced in the tumor microenvironment mainly by macrophages, endothelial cells and tumor cells[19]. It is a multifunctional cytokine that exerts cytotoxic, cytostatic and immune-modulatory effects on malignant tumors. However, the use of TNF-α in therapy is limited by its systemic toxicity. Recently, researchers have produced mhTNF-α, which is an efficient, low-toxicity TNF-α allosteric body that has good prospects in tumor treatment[13]. In our study, we demonstrated that DCs with mhTNF-α containing CRAds enhanced the inhibition of tumor growth and promoted the survival of tumor-bearing animals. Moreover, the spleen T lymphocyte CD4$^+$/CD8$^+$ ratio from prostate cancer-bearing mice was partially augmented by DCs with mhTNF-α containing CRAds. Therefore, we suspected that mhTNF-α might play a role in immune activation.

In conclusion, this work provides evidence that DCs could serve as a "Trojan horse" for CRAd delivery in anti-cancer therapy; also, CRAd-loading DCs may serve as a new treatment strategy for hormone-dependent and hormone-independent PCa.

Author contribution

Zhao-lun LI and Tie CHONG designed the research; Zhao-lun LI and Xuan LIANG performed the research; He-cheng LI contributed to the analytic tools; He-cheng LI and Zi-ming WANG analyzed the data; Zhao-lun LI and Xuan LIANG wrote the paper.

References

1   Siegel R, Naishadham D, Jemal A. Cancer statistics, 2013. CA Cancer J Clin 2013; 63: 11–30.

2   Djavan B, Moul JW, Zlotta A, Remzi M, Ravery V. PSA progression following radical prostatectomy and radiation therapy: new standards in the new Millennium. Eur Urol 2003; 43: 12–27.

3   Jeet V, Tevz G, Lehman M, Hollier B, Nelson C. Elevated YKL40 is associated with advanced prostate cancer (PCa) and positively regulates invasion and migration of PCa cells. Endocr Relat Cancer 2014; 21: 723–37.

4   Schenk E, Essand M, Bangma CH, Barber C, Behr JP, Briggs S, *et al.* Clinical adenoviral gene therapy for prostate cancer. Hum Gene Ther 2010; 21: 807–13.

5   Cheng WS, Dzojic H, Nilsson B, Totterman TH, Essand M. An oncolytic conditionally replicating adenovirus for hormone-dependent and hormone-independent prostate cancer. Cancer Gene Ther 2006; 13: 13–20.

6   Ilett EJ, Prestwich RJ, Kottke T, Errington F, Thompson JM, Harrington KJ, *et al.* Dendritic cells and T cells deliver oncolytic reovirus for tumour killing despite pre-existing anti-viral immunity. Gene Ther 2009; 16: 689–99.

7   Schmid MA, Harris E. Monocyte recruitment to the dermis and differentiation to dendritic cells increases the targets for dengue virus replication. PLoS Pathog 2014; 10: e1004541.

8   Xu H, Cao X. Dendritic cell vaccines in cancer immunotherapy: from biology to translational medicine. Front Med 2011; 5: 323–32.

9   Moodycliffe AM, Shreedhar V, Ullrich SE, Walterscheid J, Bucana C, Kripke ML, *et al.* CD40-CD40 ligand interactions *in vivo* regulate migration of antigen-bearing dendritic cells from the skin to draining lymph nodes. J Exp Med 2000; 191: 2011–20.

10 Pesonen S, Diaconu I, Kangasniemi L, Ranki T, Kanerva A, Pesonen SK, *et al.* Oncolytic immunotherapy of advanced solid tumors with a CD40L-expressing replicating adenovirus: assessment of safety and immunologic responses in patients. Cancer Res 2012; 72: 1621–31.

11 Baley PA, Yoshida K, Qian W, Sehgal I, Thompson TC. Progression to androgen insensitivity in a novel *in vitro* mouse model for prostate cancer. J Steroid Biochem Mol Biol 1995; 52: 403–13.

12 Williams BJ, Bhatia S, Adams LK, Boling S, Carroll JL, Li XL, *et al.* Dendritic cell based PSMA immunotherapy for prostate cancer using a CD40-targeted adenovirus vector. PLoS One 2012; 7: e46981.

13 Yan Z, Zhao N, Wang Z, Li B, Bao C, Shi J, *et al.* A mutated human tumor necrosis factor-alpha improves the therapeutic index *in vitro* and *in vivo*. Cytotherapy 2006; 8: 415–23.

14 Huang JH, Zhang SN, Choi KJ, Choi IK, Kim JH, Lee MG, *et al.* Therapeutic and tumor-specific immunity induced by combination of dendritic cells and oncolytic adenovirus expressing IL-12 and 4-1BBL. Mol Ther 2010; 18: 264–74.

15 Wu H, Kumar A, Miao H, Holden-Wiltse J, Mosmann TR, Livingstone AM, *et al.* Modeling of influenza-specific CD8^{+} T cells during the primary response indicates that the spleen is a major source of effectors. J Immunol 2011; 187: 4474–82.

16 Liu B, Woltman AM, Janssen HL, Boonstra A. Modulation of dendritic cell function by persistent viruses. J Leukoc Biol 2009; 85: 205–14.

17 Kim HP, Lee YS, Park JH, Kim YJ. Transcriptional and epigenetic networks in the development and maturation of dendritic cells. Epigenomics 2013; 5: 195–204.

18 Wolters T, Roobol MJ, van Leeuwen PJ, van den Bergh RC, Hoedemaeker RF, van Leenders GJ, *et al.* Should pathologists routinely report prostate tumour volume? The prognostic value of tumour volume in prostate cancer. Eur Urol 2010; 57: 821–9.

19 Bemelmans MH, van Tits LJ, Buurman WA. Tumor necrosis factor: function, release and clearance. Crit Rev Immunol 1996; 16: 1–11.